

Traffic data Collection Using Thermal Camera under Varying Lighting and Temperature Conditions in Multimodal Environments

Ting Fu, PhD Candidate; Joshua Stipancic, PhD Candidate; Luis Miranda-Moreno, Associate Professor
Department of Civil Engineering and Applied Mechanics, McGill University
Sohail Zangenehpour, Post-doc Researcher, Brisk Synergies
Nicolas Saunier, Associate Professor, Department of Civil, Geological and Mining Engineering,
Polytechnique Montréal

Paper prepared for presentation
at the NEXT GENERATION TRANSPORTATION MANAGEMENT CENTERS Session

of the 2016 Conference of the
Transportation Association of Canada
Toronto, ON

Acknowledgements:

Funding for this project was provided in part by the McGill Engineering Doctoral Award and the Natural Sciences and Engineering Research Council. The authors wish to thank Asad Lesani for his assistance in developing the thermal camera system.

ABSTRACT

Vision-based monitoring systems using visible-spectrum (regular) video cameras can complement or substitute conventional sensors and provide rich positional and classification data. Recently, new camera technologies, including thermal video sensors, have become available and may improve the performance of digital video-based sensors. However, the performance of thermal cameras under various lighting and temperature conditions has rarely been evaluated at multimodal facilities including urban intersections, where road user classification is required. The purpose of this research is to integrate existing tracking and classification computer-vision methods for automated data collection and to evaluate the performance of thermal video sensors under varying lighting and temperature conditions. The evaluation is based on the detection, classification, and speed measurements of road users. For this purpose, thermal and regular video data was collected simultaneously under different conditions across multiple sites. Among the main findings, the results show that the regular-video sensor only narrowly outperformed the thermal sensor during daytime conditions. However, the performance of the thermal sensor is significantly better for low visibility and shadows conditions, in particular for pedestrian and cyclist data collection. Interestingly, the thermal video performs acceptably during daytime, with a miss rate around 5 %. This paper also shows the importance of retraining the algorithm on thermal data with an improvement in the global accuracy of 48 %. Moreover, speed measurements by the thermal camera were consistently more accurate than for the regular video at daytime and nighttime. The thermal videos are insensitive to lighting interference and pavement temperature, and solve the issues associated with visible light cameras for traffic data collection, especially for locations with pedestrians and cyclists. In addition, thermal sensors offer other benefits such as privacy, insensitivity to glare, storage space and lower processing requirements.

Key words: thermal camera, infrared, computer vision, feature-based tracking, validation, data collection, confusion matrix

INTRODUCTION AND LITERATURE

In transportation management, planning, and road safety, collecting data for both motorized and non-motorized traffic is necessary (Robert, 2009). Collecting vehicle data was traditionally limited to manual data collection or inductive loops at fixed locations (Bahler et al., 1998), to the point that loops became standard in many jurisdictions and are still widely used today (Coifman, 2005). However, traditional loops do not provide any spatial coverage, and do not capture all road user types (loop detectors exist for bicycles but do not count vehicles or pedestrians). Trajectory data for all users (pedestrians, bicycles, and vehicles) is essential to understand microscopic behavior and surrogate safety analysis in critical road facilities such intersections with high non-motorized traffic volumes (Zangenehpour et al., 2016). These factors have spurred the development of non-intrusive traffic sensors of which video-based devices are among the most promising (Robert, 2009). Vision-based monitoring systems are widely used in ITS applications (Yoneyama et al., 2005), can complement or substitute conventional sensors (Cho & Rice, 2006), enable multiple lane detection (Bahler et al., 1998), and provide rich positional and classification data (Zangenehpour^a et al., 2015) beyond the capabilities of traditional devices (Iwasaki et al., 2013).

These benefits notwithstanding, there are several critical limitations associated with using regular video cameras, also referred to as visible spectrum video cameras, for traffic data collection. As these cameras rely on the visible light spectrum, the accuracy of detection, tracking, and classification is “sensitive to environmental factors such as lighting, shadow, and weather conditions” (Yoneyama et al., 2005; Fu et al., 2015). Perhaps the greatest limitation of regular cameras is varied performance in low light conditions and darkness (Sangnoree & Chamnongthai, 2009). Considering detection and classification at nighttime, “the light sensitivity and contrast of the camera ... are generally too weak” (Robert, 2009) to compensate for “the interference of illumination and blurriness” (Thi et al., 2008). This is particularly problematic because the increased injury risk associated with nighttime conditions leads to more, and more severe, road traffic crashes (Huang et al., 2000). During daytime, shadows and glare degrade the accuracy of extracted data (Yoneyama et al., 2005; Iwasaki et al., 2013). This is why typical computer vision approaches developed for daytime surveillance may not work under all conditions (Robert, 2009), and the advancement of vision-based traffic sensors is a pressing matter (Iwasaki et al., 2013).

Recently, new camera (sensor) technologies, including thermal or infrared sensors for traffic surveillance, have become available. Although the present cost of these cameras has prevented their widespread use in traffic analysis, cost will continue to decrease as the technology advances. Recognizing that it “is difficult to cope with all kinds of situations with a single approach” (Yoneyama et al., 2005), the performance of thermal cameras must be compared to regular cameras across varied lighting and visibility conditions to satisfy the desire for an “around-the-clock” video-based traffic sensor (Iwasaki et al., 2013). In recent years, various computer vision techniques for tracking, classification, and surrogate safety analysis have been developed (Zangenehpour^b et al 2015; Saunier, Traffic Intelligence), though nearly all these methods were developed and tested using regular video cameras. It is unclear if these methods can be directly applied to thermal video and whether thermal cameras offer a performance advantage compared to regular cameras across lighting and temperature conditions.

The purpose of this study is i) to integrate existing tracking and classification computer-vision methods for automated thermal-video data collection under low visibility conditions, nighttime and shadows and ii) to evaluate the performance of thermal video sensors under varying lighting and temperature conditions compared to visible light cameras. Performance is evaluated with respect to road user detection, classification, and vehicle speed measurements. Lighting and temperature conditions where each camera outperformed the other are identified to provide practical recommendations for the implementation of video-based sensors.

LITERATURE REVIEW

The difficulties associated with collecting traffic data using regular cameras, and attempts to rectify these issues, have been well documented in the existing literature, though many existing studies do not appropriately report performance, be it for detection, classification, or tracking. Yoneyama et al. (2005) demonstrated that nighttime detection misses are up to 50 % and false alarms are 3.4 % of the ground truth total, much higher than for daytime detection. Robert (2009) showed that vehicle counts were accurate in various lighting, weather, and traffic conditions when using a headlight detection method, although sample sizes were generally 100 vehicles or less. Methods that detect headlights or taillights are typically only applicable at night, and the headlight detection method may increase the difficulty of vehicle classification (Iwasaki et al., 2013). Thi et al. (2008) proposed a methodology using eigenspaces and machine learning for classification from regular video at nighttime. The authors found a successful classification rate of 94 % compared to 70 % or lower for other classification schemes. Coifman et al. (1998) suggested that “to be an effective traffic surveillance tool ... a video image processing system ... should ... function under a wide variety of lighting conditions”. The authors proposed feature-based tracking as an improvement over those methods dependent on identifying an entire vehicle, because even under different lighting or visibility conditions, “the most salient features at the given moment are tracked” (Coifman et al., 1998). The proposed algorithm was evaluated on highways where it was generally successful at tracking vehicles in congestion, shadow, and varying lighting conditions.

With the limited success of regular cameras in adverse conditions, many researchers have considered alternative technologies for traffic data collection. Balsys, Valinevicius, and Eidukas (2009) identified that weather interference could be avoided using infrared (thermal) cameras, demonstrating that the cameras eliminated issues associated with headlight glare at night and cast shadows during the day. Thermal video demonstrated a 15 % improvement in detection rate over visible light cameras. Sangnoree and Chamnongthai (2009) presented a method for detecting, classifying, and measuring speeds of vehicles at night using thermal videos. Although classification and speed estimation were successful, detection worked best when only a single vehicle was present in the video frame (84 % success) but suffered when two or more vehicles were present (41-76 % success). Iwasaki (2008) developed a vision-based monitoring system that works robustly around-the-clock using infrared thermography. Iwasaki et al. (2013) achieved 96 % successful detection of vehicles using thermal video in poor visibility conditions. MacCarley et al. (2000) compared several infrared and visible light cameras, and found that many infrared cameras were “virtually immune to headlight or streetlight backscatter” and therefore performed best in darkness, fog, or the combination of darkness and fog. However, without fog or with light fog, the visible light camera outperformed infrared cameras, and “there appears to be a limited number of situations for which non-visible spectrum imaging appears to be justified”, including dense fog or scenes with glare or shadows (MacCarley et al., 2000).

Thermal video has been used successfully for nighttime pedestrian detection, an area of particular importance because pedestrians may be less visible to drivers at night, and are therefore at a greater risk of collision (Huang et al., 2000). Xu et al. (2005) used a support vector machine (SVM) to detect and classify pedestrians using a thermal camera mounted to a moving vehicle. Although detection was successful in many cases, occlusion of pedestrians in heavy traffic was a significant limitation. Krotosky and Trivedi (2007) analyzed multiple camera technologies. Recognizing that regular and thermal cameras provide “disparate, yet complementary information about a scene”, the authors recommend combining visible light and infrared technologies (Krotosky & Trivedi, 2007).

Despite this existing work, several shortcomings exist. Although several studies have addressed detecting vehicles or pedestrians, there has been limited work on detecting and classifying multiple road user types (including bicycles) from thermal video in mixed-traffic environments such as urban intersections. No studies have attempted to identify the effect of pavement temperature on the quality

of thermal video. Although thermal video sensors are promising, their performance must be comprehensively evaluated and the adaptation of existing computer vision software must be studied. Most studies do not appropriately report performance and cannot be reproduced since the software code and/or datasets are not available. Detection rate alone is too limited to represent performance. The whole confusion matrix should be presented and receiver operating characteristic (ROC) curves should be used to evaluate detectors or classifiers as parameters are adjusted. Separate data sets for calibration and performance measurements should be required. When available, researchers should use standard metrics such as the Measure of Tracking Accuracy (MOT) (Bernardin & Stiefelhagen, 2008). This research aims to address these gaps and integrate thermal sensors into existing data collection and safety tools, in particular under conditions where regular video presents limitations.

METHODOLOGY

The methodology considers three steps: i) technology integration and data collection, ii) implementation of detection and classification algorithms, and iii) vehicle speed validation.

Technology Integration and Data Collection

The two technologies involved in this study are thermal-video sensors with a resolution of 368×296 pixels and visible-light cameras with a resolution of 1920×1080 pixels. The thermal camera system consists of a thermal sensor, a signal converter, and a power supply unit. Thermal video data is stored on a simple chip microcomputer (SCM). The thermal sensor, the ThermiCam by FLIR, is connected to an X-stream edge card that reads, converts, and outputs the thermal signal to a video file. The video file is then transferred to the SCM using an Ethernet connection where it is saved using the VLC Software (VideoLAN Organization). The camera and X-stream edge card are powered using a battery with an 12-24 V output. The SCM, the battery and the X-stream edge card are placed in a small enclosure which can be easily installed for data collection. FIGURE 1 presents the components of the thermal camera system and a sample frame from the thermal camera recorded at night in FIGURE 1c.

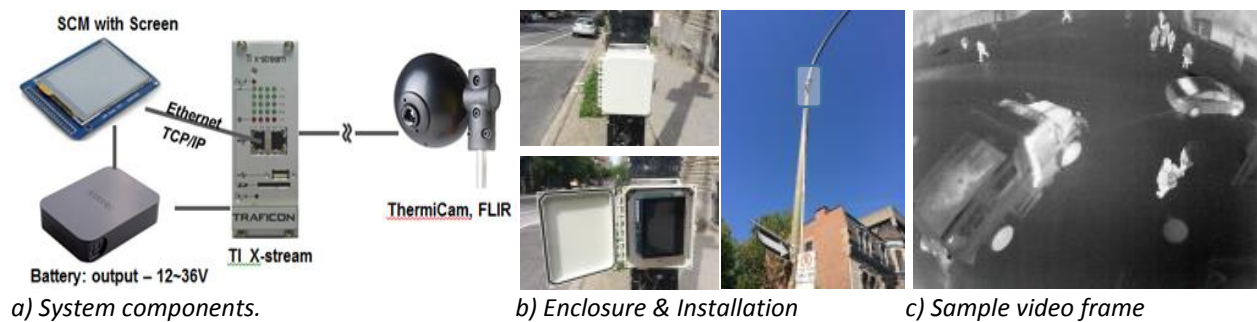


FIGURE 1 Thermal camera system*¹

Three primary sources of data are required: thermal video data, visible spectrum video data, and environmental and pavement temperature data. The regular visible-spectrum camera and thermal camera systems are installed simultaneously using a telescoping-fibreglass mast to ensure nearly identical fields of view. The regular camera system, as introduced in (Zangenehpour^b et al., 2015), uses an inexpensive and commercially available video camera which stores video and is powered internally.

¹ Note that in the field, the battery, SCM and the TI X-stream are enclosed in a small waterproof case.

Since the road pavement is the primary background in the video scenes, pavement temperature is regarded as the main temperature variable affecting thermal video performance. Pavement temperature data were collected using the FLIR ONE thermal camera (FLIR Systems, Inc., 2015), which attaches to an iPhone to capture thermal video and temperatures using the FLIR ONE iPhone application. The camera was held close to the road surface to get the temperature as suggested in the user manual (FLIR Systems, Inc., 2014). Based on field-testing, the temperature measured by the FLIR ONE was within 2°C of the actual pavement temperature.

Implementation of Detection and Classification Algorithms

As thermal videos detect thermal energy, they are expected to solve the issues associated with visible light cameras under different lighting conditions. Existing detection and classification algorithms are used for automated data collection; however they need to be re-trained and evaluated under different lighting and temperature conditions. Additional details of the methods for detection, tracking and classification are presented in the next sub-sections.

Detection and Tracking Algorithm

The videos were processed using the tracker available in Traffic Intelligence, an open-source computer-vision software project (Saunier & Sayed, 2006). Individual pixels are first detected and tracked from frame to frame, and recorded as feature trajectories using the Kanade-Lucas-Tomasi feature tracking algorithm (Shi & Tomasi, 1994). Feature trajectories are then grouped based on consistent common motion to identify unique road users. The techniques used in the tracker are further explained by Shi and Tomasi (Shi & Tomasi, 1994) and Saunier and Sayed (Saunier & Sayed, 2006). Algorithm parameters were calibrated through trial and error, in order to minimize both false alarms and misses. False alarms and misses respectively result mostly from over-segmentation (one user being tracked as multiple users) and over-grouping (multiple users being tracked as one user).

Classification Algorithm and Algorithm Retraining

Road user classification was performed using the method developed by Zangenehpour, Miranda-Moreno, and Saunier (Zangenehpour^a et al., 2015). Classifier V classifies detected road users as vehicles, pedestrians, or cyclists based on the combination of appearance, aggregate speed, speed frequency distribution and location in the scene. A SVM is used to learn the appearance of each road user type as described by the well-known Histogram Oriented Gradients (HoG). The SVM was trained based on a database containing 1500 regular images of each road user type. The overall accuracy of this classification method at intersections with high volumes and mixed road user traffic is approximately 93 %, an improvement over simpler algorithms using only one or two classification cues (Zangenehpour^a et al., 2015). The classifiers are available in Traffic Intelligence (Saunier, Traffic Intelligence). For more details regarding the original classification method, readers are referred to (Zangenehpour^a et al., 2015).

Considering that the classifier uses the appearance of the road user as a parameter, and the fact that road users in thermal videos appear quite differently than they do in visible light videos, the SVM classifier for appearance classification, as part of the Classifier V (Zangenehpour^a et al., 2015) that is used in this study, needs to be retrained on a dataset of thermal images for all road user types. Although the shape and proportions of the road users should be roughly equivalent, it is unclear how their appearance described by HOG varies between the visible and thermal images. Furthermore, the reduced resolution of the thermal video may impact the classification performance as less information and fewer details are available. The accuracy of the classification algorithm must therefore be explored further. This study used a database containing 1500 thermal images from several videos (separate from the

videos used for performance evaluation) for each type of road user to train the SVM and compared the classification rate using the SVM trained respectively on the regular and the thermal dataset.

Detection and Classification Performance Metrics

The detection and classification performance are measured using different metrics and by extracting video data from frames every 10 seconds. This corresponds to 150 frames considering a frame rate of 15 frames per second, fps). Data (detection, user class and speed) is then extracted by observing the results of the tracking and classification algorithms and compared visually with the ground truth. The interval of 10 s was chosen to be large enough in order to avoid evaluating the same road user twice. Most road users are tracked less than 10 s continuously as the tracking algorithm tracks only moving road users (if stopped, a road user is not tracked anymore: tracking resumes when the road user starts moving again): trajectories are typically less than 5 s long for vehicles, and less than 10 s for pedestrians and cyclists. Also, 10 s is short enough to provide enough observations to evaluate the detection and classification performance. For each extracted frames, detection and classification errors are counted as shown in FIGURE 2.

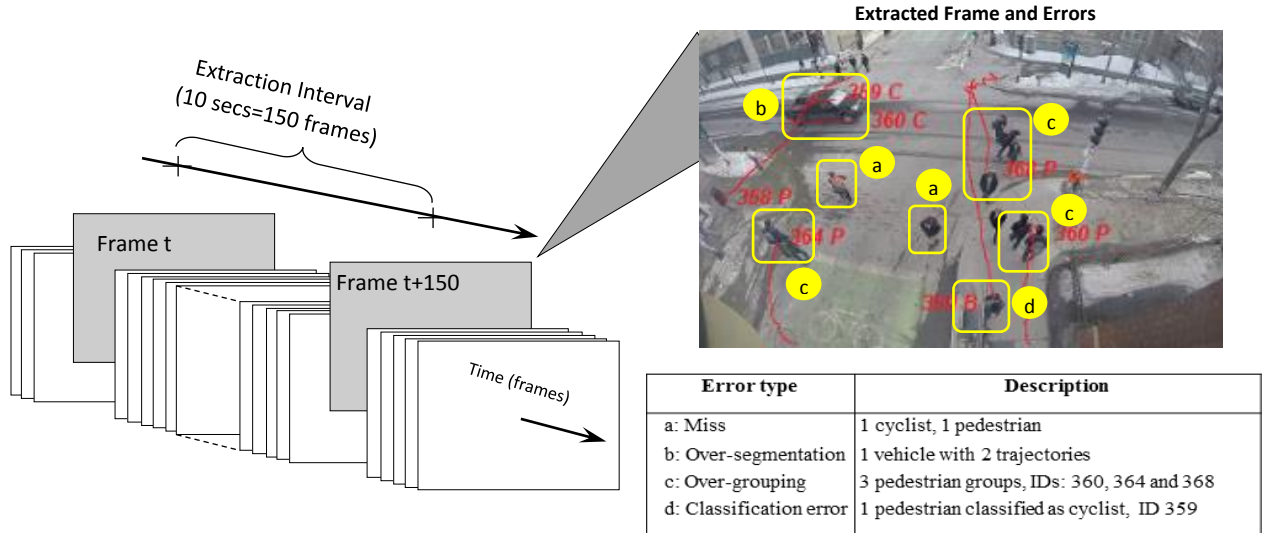


FIGURE 2 Video Sampling and Data Extraction for Detection & Classification Performance

Different metrics are computed to evaluate the performance of thermal vs regular video. For the classification problem, the confusion matrix is used to investigate the technology performance and derive metrics. In the general case with N classes, the confusion matrix is a $N \times N$ matrix that contains in each cell c_{ij} the number of objects of true class i predicted as class j . The detection & tracking step can be also evaluated as a binary classification problem (a matrix with $N=2$ classes, miss and detected), where the class of objects to be detected is the positive class. The matrix in this binary case is presented in TABLE 1 with the particular names taken by the instances depending on their true and predicted class. Misses are the false negatives and false alarms are the false positives.

The most common metric is the global accuracy defined as the proportion of correct predictions:

$$Accuracy = \frac{\sum_k c_{kk}}{\sum_i \sum_j c_{ij}} \quad (1)$$

The majority of existing studies have used global accuracy to measure classification performance, both

for road user detection and classification methods. This is however insufficient to properly report the performance, both for two-class classification, i.e. detection (since false alarms are not accounted for by a single detection rate) and for classification with three and more classes such as in multimodal environments, e.g. with pedestrians, cyclists, and vehicles. As used widely in the field of machine learning, this study relied on the confusion matrix to derive the following disaggregate metrics per class:

$$Precision_k = \frac{C_{kk}}{\sum_i C_{ik}} \quad (2)$$

$$Recall_k = \frac{C_{kk}}{\sum_j C_{kj}} \quad (3)$$

In the case of a binary classification problem, precision and recall are typically reported only for the positive class, and can be written in terms of true/false positives/negatives as follows:

$$Precision = \frac{TP}{TP+FP} = \frac{c_{11}}{c_{11}+c_{21}} \quad (4)$$

$$Recall = \frac{TP}{TP+FN} = \frac{c_{11}}{c_{11}+c_{12}} \quad (5)$$

From which, the miss rate can be derived as, $miss\ rate = 1 - Recall = \frac{FN}{TP+FN}$;

The above metrics are computed by populating the confusion matrix through the visual assessment of each frame every 10 s or 150 frames as shown in FIGURE 2. Since pedestrians often move in groups, and detecting and tracking individual pedestrians within groups is difficult (and actually an open problem in all conditions in computer vision), the unit of analysis is individual pedestrians or groups of pedestrians. In FIGURE 2, the groups of pedestrians labeled c (over-grouping) is then considered correctly detected. Miss rate is the main metric reported for detection performance used for all test cases in the experimental results, while precision and recall at the individual level, overall and per known (true) type of road user, are also reported for two test cases for a more complete assessment.

The road user classification problem has three classes: pedestrians, cyclists and vehicles. Precision and recall are reported for each class, as well as global accuracy, from the confusion matrix accumulated over all frames used for performance evaluation.

TABLE 1 Corresponding Table of Confusion & Basic Terms from Confusion Matrix

		Predicted class		
		Positive	Negative	
True class	Positive	True Positives (TP)	False Negatives (FN)	$Recall = \frac{TP}{TP + FN}$
	Negative	False Positives (FP)	True Negatives (TN)	
		$Precision = \frac{TP}{TP + FP}$		

Vehicle Speed Validation

Once road users have been detected and classified, parameters such as vehicle speed are of interest for traffic studies. Many existing studies have used mean relative error (MRE) to quantify the error of video speeds extracted automatically from video. However, a previous study by Anderson-Trocmé et al. (2015) showed that it “is insufficient at capturing the true behaviour of detectors and other measures are

necessary to define device precision and accuracy separately”, where accuracy is the systematic error or bias, and precision is the residual error. However, because video-based sensors tend to overestimate speed, and because this overestimation is roughly constant with respect to speed, simple methods for calculating relative precision error and relative accuracy error were developed.

The vehicle speed validation process begins by plotting automatically extracted speeds against manually measured speeds (speeds calculated based on known distances and video frame rate) in order to observe trends across visibility and temperature conditions. The line $y=x$ represents ideal detector performance, and data points above the line indicate overestimation of speed, while points below the line indicate underestimation. As the overestimation bias is typically constant, a line with slope equal to one is fitted to the data. The y-intercept and R-squared values of this fitted line represent accuracy and precision respectively. However, converting these results to relative error values “matches the approach utilized in existing literature, and provides an intuitive and communicable comparison” between multiple environments (Anderson-Trocme et al., 2015). Relative precision error (RPE) is quantified similarly to mean relative error, with the subtraction of a correction factor equal to the y-intercept of the fitted line. To normalize the intercept value consistently with the relative mean error, the y-intercept is evaluated at every data point (divided by the harmonic mean of observed speed) for the relative accuracy error (RAE). The RAE represents the over- or under-estimation bias present in the video data. The RPE can be seen as the best possible performance that could be expected from calibrated video data (Anderson-Trocme et al., 2015). Values for relative error, relative precision and accuracy error are calculated as

$$\text{Mean Relative Error (MRE)} = \frac{1}{100} \sum \frac{|V_e - V_o|}{V_o} \quad (6)$$

$$\text{Relative Precision Error (RPE)} = \frac{1}{100} \sum \frac{|(V_e - y \text{ intercept}) - V_o|}{V_o} \quad (7)$$

$$\text{Relative Accuracy Error (RAE)} = \frac{1}{100} \sum \frac{|y \text{ intercept}|}{V_o} \quad (8)$$

Where V_e and V_o stands for the automatically extracted and manually measured speeds respectively.

DATA DESCRIPTION

To evaluate the performance of the thermal and regular cameras, 14 test cases (camera installations), with approximately one to four hours of video data for each case, were used. The lighting test cases, presented in TABLE 2, include videos during the day and at night. Daytime test cases focussed on various sun exposures and shadow conditions, while nighttime test cases focussed on the level of visibility, with one case in near complete darkness, one nearly completely illuminated, and one in between. Speed performance was evaluated on a sample size of 100 vehicles for each test case, while classification and detection performance was evaluated on 30 minutes of sample videos.

A similar approach was adopted for the temperature test cases, shown in TABLE 3. To evaluate detection and classification performance under different temperature conditions, thermal video data were collected from the same site with the same camera angle throughout a sunny summer day when the pavement temperature rose from 20°C in the morning to 50°C in the afternoon. Data collected from the same site in winter when the pavement temperature was close to 0°C was included. As with the lighting test cases, speed performance was evaluated on a 100-vehicle sample, and classification and detection performance was evaluated on 20 minute video samples. In TABLE 3, the thermal images change drastically from cold to hot pavement temperature. Road users are light on a dark background when the pavement temperature is low, and dark on a light background when the temperature is high.

TABLE 2 Summary of Lighting Test Cases

Lighting Condition		VEHICLE SPEED			CLASSIFICATION		
		Sample Size	Season	Road Type	Video Length	Season	Road type
Daytime	Overcast	100 vehicles	Winter	Segment	Every 10 s for 30 minutes	Summer	Intersection
	Sun, little shadow		Spring			Summer	Intersection
	Sun, slight shadows		Spring			N/A	N/A
	Sun, strong shadows		Summer			Summer	Intersection
Nighttime	High visibility	100 vehicles	Spring	Segment	Every 10 s for 30 minutes	Winter	Intersection
	Medium visibility			Intersection			
	Low visibility			Intersection			

SAMPLE CAMERA VIEWS UNDER DIFFERENT LIGHTING CONDITIONS




















Daytime Conditions	Thermal Camera	Regular Camera	Nighttime Conditions	Thermal Camera	Regular Camera
Overcast			High visibility		
Sun, little shadow			Medium visibility		
Sun, strong shadows			Low visibility		

TABLE 3 Summary of Temperature Test Cases

Pavement Temp.	Ambient Temp.	Sample Size	Season	Road Type
VEHICLE SPEED				
0 °C- 5°C	~ 0 °C	100 vehicles	Winter	Segment
20 °C-25°C	~ 20 °C		Summer	Segment
25 °C-30°C	~ 20 °C		Summer	Segment
30 °C-35°C	~ 20 °C		Summer	Segment
35 °C-40°C	~ 20 °C		Summer	Segment
40 °C-45°C	~ 20 °C		Summer	Intersection
CLASSIFICATION				
0 °C- 5°C	~ 0 °C	Every 10 s (150 frames) for 20 minutes	Winter	Intersection
20 °C-25°C	~ 20 °C		Summer	
25 °C-30°C	~ 20 °C		Summer	
30 °C-35°C	~ 20 °C		Summer	
35 °C-40°C	~ 20 °C		Summer	
40 °C-45°C	~ 20 °C		Summer	
45 °C-50°C	~ 20 °C		Summer	
SAMPLE CAMERA VIEWS UNDER DIFFERENT TEMPERATURE				
Pavement Temp.	Camera View	Pavement Temp.	Camera View	
0°C- 5°C		35°C-40°C		
20°C-25°C		40°C-45°C		
25°C-30°C		45°C-50°C		
30°C-35°C				

RESULTS

Detection and Classification

Lighting

Results of detection and classification for the thermal and regular video are presented in TABLE 4 for the lighting test cases. The thermal camera reported a miss rate of 5 % or less for all road user types in nearly all test cases. While the vehicle miss rate of the regular camera was also lower than 5 % in all test cases, the rate increased significantly for pedestrians and cyclists in all nighttime test cases, where very few pedestrians and cyclists were detected with the regular camera (more than 75 %). Vehicles were well detected by both technologies under all conditions, possibly because their lit headlights and larger size provide more features for tracking compared to pedestrians and cyclists. In conditions without interference of darkness or shadows (test cases of “overcast” and “sun, little shadow”), excellent performance was obtained for the regular videos. However, daytime cases with shadows showed a decrease in performance, as shadows inhibit the tracking and detection of pedestrians, cyclists, and some vehicles. The miss rates of pedestrians and cyclists both increased to around 15 %, 10 % points higher than those in the thermal videos.

For classification performance, the measures of recall and precision are also presented in TABLE 4. Higher values of recall and precision in classifying vehicles using regular videos indicate that, in general, the performance of classifying vehicles was improved when using the regular camera over the thermal camera. However, from medium to low visibility conditions, regular cameras perform poorly in the classification of cyclists and pedestrians. For cases with medium and low visibility specifically, the algorithm failed to recognize pedestrians and cyclists in regular videos. In such cases, since classification is performed only for tracked road users, computing the precision may not be possible when no road user of the class was detected or representative if too few were detected. Thermal videos perform reliably in nighttime cases, even when using the classification algorithm trained on the regular, or visible spectrum, images of road users. In daytime conditions, the classification of pedestrians and cyclists is only slightly better by regular camera, as the global accuracy values are slightly higher in regular videos than those in thermal videos in most cases. The classification performance per class indicates the need for improving the classification algorithm for thermal videos by training the algorithm on images from thermal cameras. Nevertheless, even with the algorithm trained only on regular video data, the thermal camera correctly classifies road users more often in low visibility conditions, especially at nighttime.

A more complete detection performance evaluation, in particular for individual pedestrians, is reported for two extreme test cases: i) the sunny daytime case without the interference of shadow, which has the best lighting environment, presented in TABLE 5, and, ii) the worst lighting condition case shown in TABLE 5, which is nighttime condition with low visibility. From the results, the thermal camera and the regular camera perform similarly well in detecting different road users in the good lighting environment. For low visibility condition at night, the two camera systems have similar capability in detecting vehicles; however, the regular camera failed to detect the cyclists and pedestrians under such a low visibility condition (low recall) where the thermal camera can still work efficiently – this is in accordance with the previous analysis. With similar performance for good lighting conditions and much better performance for low visibility conditions, compared to the visible spectrum camera system, thermal cameras can be used for all weather and lighting conditions.

1
2

TABLE 4 Detection and Classification Performance for Different Lighting Conditions – Thermal and Regular Video

Lighting Condition		THERMAL VIDEO				REGULAR VIDEO			
		No. of Presence	No. of Missed/ Miss Rate	Classification Precision	Classification Recall	No. of Presence	No. of Missed/ Miss Rate	Classification Precision	Classification Recall
Vehicle Detection and Classification									
Daytime	Overcast	121	0 / 0.0 %	53.3 %	97.0 %	192	0 / 0.0 %	78.9 %	99.3 %
	Sun, little shadow	52	2 / 3.8 %	46.3 %	100.0 %	74	0 / 0.0 %	67.9 %	100.0 %
	Sun, strong shadows	77	0 / 0.0 %	44.2 %	100.0 %	83	3 / 3.6 %	55.0 %	100.0 %
Nighttime	High visibility	102	1 / 1.0 %	66.7 %	91.2 %	102	4 / 3.9 %	74.5 %	97.6 %
	Medium visibility	249	4 / 1.6 %	99.0 %	96.2 %	241	11 / 4.6 %	97.2 %	99.5 %
	Low visibility	42	1 / 2.4 %	56.3 %	96.4 %	42	2 / 4.8 %	91.4 %	100.0 %
Cyclist Detection and Classification									
Daytime	Overcast	26	1 / 3.8 %	36.1 %	81.3 %	38	1 / 2.6 %	30.9 %	96.7 %
	Sun, little shadow	46	1 / 2.2 %	95.8 %	54.8 %	57	4 / 7.0 %	87.8 %	78.3 %
	Sun, strong shadows	68	4 / 5.9 %	90.3 %	50.0 %	67	11 / 16.4 %	63.0 %	68.0 %
Nighttime	High visibility	44	1 / 2.3 %	70.2 %	93.0 %	44	36 / 81.8 %	42.9 %	37.5 %
	Medium visibility	12	0 / 0.0 %	64.7 %	100.0 %	12	12 / 100.0 %	0.0 %	Invalid
	Low visibility	10	0 / 0.0 %	69.2 %	90.0 %	10	10 / 100.0 %	Invalid	Invalid
Pedestrian Detection and Classification									
Daytime	Overcast	314	9 / 2.9 %	98.3 %	68.5 %	356	14 / 3.9 %	99.1 %	68.3 %
	Sun, little shadow	78	2 / 2.6 %	82.1 %	56.1 %	63	0 / 0.0 %	93.8 %	66.2 %
	Sun, strong shadows	118	9 / 7.6 %	100.0 %	46.8 %	130	19 / 14.6 %	86.6 %	59.2 %
Nighttime	High visibility	149	5 / 3.4 %	97.8 %	68.9 %	149	109 / 73.1 %	90.0 %	25.7 %
	Medium visibility	85	3 / 3.5 %	94.5 %	94.5 %	77	68 / 88.3 %	100.0 %	14.3 %
	Low visibility	286	4 / 1.4 %	99.5 %	89.5 %	286	278 / 97.2 %	Invalid	0.0 %
Total Detection and Classification									
Accuracy					Accuracy				
Daytime	Overcast	461	10 / 2.2 %	74.9 %		586	15 / 2.6 %	79.1 %	
	Sun, little shadow	176	5 / 1.8 %	66.2 %		194	4 / 2.1 %	80.2 %	
	Sun, strong shadows	263	13 / 4.9 %	62.8 %		280	33 / 11.8 %	69.1 %	
Nighttime	High visibility	295	7 / 2.4 %	79.4 %		295	159 / 50.5 %	74.0 %	
	Medium visibility	346	7 / 2.0 %	96.1 %		330	91 / 27.6 %	96.8 %	
	Low visibility	338	5 / 1.5 %	90.3 %		338	290 / 85.8 %	91.4 %	

TABLE 5 Detection Performance Results – Test Case: Nighttime, Low Visibility

Test Cases	Camera	Precision				Recall			
		Vehicle	Cyclist	Pedestrian	Overall	Vehicle	Cyclist	Pedestrian	Overall
Sun, little shadow	Thermal Camera	66.3 %	98.5 %	94.2 %	86.8 %	93.0 %	82.3 %	79.0 %	82.8 %
	Regular Camera	65.2 %	94.4 %	97.8 %	81.5 %	95.6 %	91.1 %	81.3 %	88.5 %
Night, low visibility	Thermal Camera	57.7 %	100 %	99.7 %	91.6 %	97.6 %	100 %	75.1 %	77.8 %
	Regular Camera	64.5 %	Invalid	88.9 %	67.6 %	95.2 %	0 %	2.1 %	11.1 %

Temperature

The classifier trained on the thermal dataset was applied in the different temperature test cases where the outputs of the thermal videos changed greatly with the change of temperature. TABLE 6 presents the results of detection and classification performance for the classifier trained on the regular or thermal dataset for each test case. Again, the thermal video provided detection rates exceeding 95 % for nearly all test cases, and temperature had little impact on detecting different road users. Even when the pavement temperature approaches that of the road users, miss rate remained low. Observing the videos, temperature variation within each road user likely explains this good performance: features are still detected for the areas of high and low temperature within road users.

Although miss rate was low, classification results were generally poor before retraining the algorithm, and classification accuracy reduced systematically as temperature increased from 90.3 % in the lowest temperature case to 30.8 % in the highest. This result indicates that, for the thermal video, the object appearance described by HoG (Zangenehpour^a et al., 2015) varies with pavement temperature, and therefore the SVM should be trained on thermal images to account for the different appearance of road users. The classification accuracy after the new training showed improvements, particularly at higher pavement temperatures. At 45-50 °C, overall classification accuracy improved by 48.6 % points –from accuracy of 30.8 to 79.4 %. The excellent performance of detection and the higher classification accuracy rates for the algorithm trained on thermal data indicate the possibility of using this algorithm to correctly detect and classify different types of road users under different temperature conditions.

Looking at the per-class performance measures, better recall and precision were found in almost all temperature cases for vehicles and pedestrians when using the algorithm trained with thermal data (with an average increase of 26.3 % points in precision for vehicles, and an average increase of 24.1 % points in recall and 22.2 % points in precision for pedestrians). The recall for cyclists increases in all cases by 39.5 % points on average; however, precision decreases in most of the cases by 10.1 % points on average. This is explained by considering that, before training the algorithm on thermal data, a smaller portion of the detected cyclists are successfully classified which leads to a deceptively high precision. In other words, fewer cyclists were classified as such by the algorithm trained with regular videos, but the algorithm made few mistakes, and the other cyclists were classified as pedestrians or vehicles resulting in lower precision for these road user types. With a the newly trained algorithm, more road users, including actual cyclists are classified as cyclists, which increases cyclist recall; but in doing so, more vehicles and pedestrians are also misclassified as cyclists, causing a decrease in cyclist precision. A general issue for both types of cameras is confusing pedestrians and cyclists since they have similar appearances. Global accuracy improved by as much as 50 % points in the multimodal environments. Moreover, the % point improvement was larger for high temperature cases, indicating that training the algorithm for data collection using thermal videos is both necessary and effective.

TABLE 6 Detection and Classification Performance for Different Pavement Temperatures – Thermal Camera

Pavement Temp.	No. Presence	No. of Missed /Miss Rate	Classifier Trained on Regular data		Classifier Trained on Thermal data		Improvement (% points)	
			Precision	Recall	Precision	Recall	Precision	Recall
Vehicle Detection and Classification								
0 °C- 5°C	42	1 / 2.4 %	56.3 %	96.4 %	67.4 %	96.7 %	11.2 %	0.2 %
20 °C-25°C	58	0 / 0.0 %	89.1 %	100.0 %	96.1 %	100.0 %	7.0 %	0.0 %
25 °C-30°C	37	2 / 5.4 %	67.6 %	100.0 %	83.9 %	100.0 %	16.2 %	0.0 %
30 °C-35°C	20	0 / 0.0 %	27.9 %	100.0 %	68.4 %	100.0 %	40.5 %	0.0 %
35 °C-40°C	45	1 / 2.2 %	35.6 %	100.0 %	67.5 %	100.0 %	31.9 %	0.0 %
40 °C-45°C	31	1 / 3.2 %	23.6 %	100.0 %	65.4 %	100.0 %	41.7 %	0.0 %
45 °C-50°C	19	0 / 0.0 %	12.1 %	100.0 %	47.6 %	100.0 %	35.5 %	0.0 %
Average			44.6 %	99.5 %	70.9 %	99.5 %	26.3 %	0.0 %
Cyclist Detection and Classification								
0 °C- 5°C	10	0 / 0.0 %	69.2 %	90.0 %	64.3 %	100.0 %	-4.9 %	10.0 %
20 °C-25°C	33	0 / 0.0 %	72.1 %	96.9 %	64.6 %	96.9 %	-7.5 %	0.0 %
25 °C-30°C	22	0 / 0.0 %	70.0 %	46.7 %	70.8 %	94.4 %	0.8 %	47.8 %
30 °C-35°C	36	0 / 0.0 %	93.8 %	51.7 %	75.8 %	86.2 %	-18.0 %	34.5 %
35 °C-40°C	27	2 / 7.4 %	88.9 %	33.3 %	67.9 %	76.0 %	-21.0 %	42.7 %
40 °C-45°C	40	0 / 0.0 %	88.9 %	22.9 %	83.8 %	86.1 %	-5.1 %	63.3 %
45 °C-50°C	26	0 / 0.0 %	100.0 %	6.7 %	85.0 %	85.0 %	-15.0 %	78.3 %
Average			83.3 %	49.7 %	73.2 %	89.2 %	-10.1 %	39.5 %
Pedestrian Detection and Classification								
0 °C- 5°C	286	4 / 1.4 %	99.5 %	89.5 %	100.0 %	92.0 %	0.5 %	2.5 %
20 °C-25°C	71	0 / 0.0 %	100.0 %	66.0 %	100.0 %	66.7 %	0.0 %	0.7 %
25 °C-30°C	39	0 / 0.0 %	86.4 %	67.9 %	100.0 %	66.7 %	13.6 %	-1.2 %
30 °C-35°C	53	3 / 5.7 %	75.0 %	42.9 %	97.0 %	74.4 %	22.0 %	31.6 %
35 °C-40°C	51	2 / 3.9 %	62.5 %	12.5 %	96.7 %	63.0 %	34.2 %	50.5 %
40 °C-45°C	44	2 / 4.5 %	50.0 %	23.3 %	96.3 %	70.3 %	46.3 %	46.9 %
45 °C-50°C	44	2 / 4.5 %	61.1 %	33.3 %	100.0 %	71.1 %	38.9 %	37.7 %
Average			76.4 %	47.9 %	98.6 %	72.0 %	22.2 %	24.1 %
Total Detection and Classification								
			Accuracy		Accuracy		Accuracy	
0 °C- 5°C	338	5 / 1.5 %	90.3 %		92.8 %		2.6 %	
20 °C-25°C	162	0 / 0.0 %	86.3 %		85.9 %		-0.3 %	
25 °C-30°C	98	3 / 3.1 %	74.2 %		84.4 %		10.2 %	
30 °C-35°C	109	3 / 2.7 %	54.2 %		82.4 %		28.1 %	
35 °C-40°C	123	5 / 4.1 %	43.3 %		76.5 %		33.2 %	
40 °C-45°C	115	3 / 2.6 %	35.9 %		82.2 %		46.3 %	
45 °C-50°C	89	2 / 2.2 %	30.8 %		79.4 %		48.6 %	
Average			59.3 %		83.4 %		24.1 %	

Vehicle Speed Validation

To compare the performance of the camera systems in vehicle speed extraction accuracy, a data visualization exercise was completed for all test cases. One example, shown in FIGURE 3, demonstrates the performance of the two camera systems under sun with strong shadows.

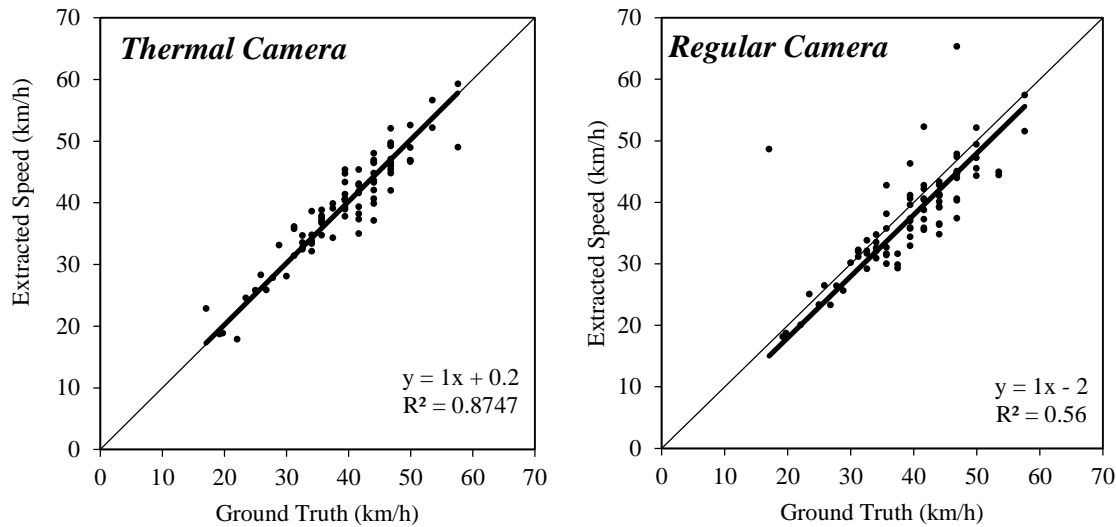


FIGURE 3 Example of vehicle speed estimation performance for thermal and regular cameras under sun with strong shadows

Speed and Lighting

TABLE 7 provides the equation of the fitted line, its R-squared value, MRE, RAE, and RPE for each lighting conditions test case. The first important observation was that the intercept value in nearly all test cases was positive for both technologies. This result is consistent with previous research and shows that video sensors tend to overestimate speeds (Anderson-Trocme et al., 2015). The R-square values for thermal video are significantly higher for daytime with shadows as well as median and low visibility conditions. RPE is perhaps the most critical values in TABLE 7. The thermal camera had a lower RPE in all test cases other than overcast sky, in which the regular camera was expected to perform well without lighting interference. In the other test cases, the thermal video consistently provided a 2-3 % points improvement in RPE over the regular camera. Despite this good performance, the RAE was highly variable both across conditions and across cameras. This again supports previous research, and indicates that the overestimation bias is less a function of camera or conditions as it is a function of user calibration error (Anderson-Trocme et al., 2015). In general, the RPE was within 5-10 % of ground truth, which is consistent with previously measured performance of video sensors (Anderson-Trocme et al., 2015).

Speed and Temperature

Similarly for the temperature test cases, parameters of the fitted line and the segregated relative errors values are presented in TABLE 8. The RPE for all but one test case was 0.06 or less, and was not observed to vary greatly with temperature. For one test case (35-40°C), several outliers greatly increased the reported error. A slight increase in RPE was noted between 20 and 30°C. These pavement temperatures

most closely match the surface temperature of vehicles, and so a slight performance decrease may be explained by tracking issues associated with the low contrast associated with the pavement temperature. Despite the slight effect of temperature, the thermal videos performed reliably and consistently across all temperature test cases, with errors equal to what is expected from existing research. Thermal videos can be an effective substitute for regular videos with regards to speed data extraction under various lighting and temperature conditions.

TABLE 7 Vehicle Speed Performance for Different Lighting Conditions – Thermal and Regular Video

		THERMAL VIDEO		REGULAR VIDEO	
Lighting Condition		Calibration Model	R ²	Calibration Model	R ²
Daytime	Overcast	$y = x - 1.97$	0.91	$y = x - 0.04$	0.95
	Sun, little shadow	$y = x + 2.91$	0.96	$y = x + 1.77$	0.92
	Sun, slight shadows	$y = x + 2.50$	0.93	$y = x + 5.75$	0.90
	Sun, strong shadows	$y = x + 0.20$	0.88	$y = x - 2.00$	0.56
Nighttime	High visibility	$y = x + 4.49$	0.93	$y = x + 0.01$	0.92
	Medium visibility	$y = x + 2.45$	0.86	$y = x + 4.14$	0.46
	Low visibility	$y = x + 0.17$	0.97	$y = x + 0.83$	0.93

		THERMAL VIDEO			REGULAR VIDEO		
Lighting Condition		MRE	RAE	RPE	MRE	RAE	RPE
Daytime	Overcast	0.067	0.058	0.067	0.059	0.001	0.059
	Sun, little shadow	0.106	0.116	0.045	0.069	0.071	0.062
	Sun, slight shadows	0.103	0.105	0.047	0.226	0.242	0.063
	Sun, strong shadows	0.061	0.005	0.061	0.108	0.053	0.097
Nighttime	High visibility	0.150	0.151	0.047	0.051	0.000	0.051
	Medium visibility	0.104	0.082	0.072	0.150	0.138	0.104
	Low visibility	0.036	0.026	0.033	0.060	0.005	0.059

TABLE 8 Vehicle Speed Performance for Different Pavement Temperature – Thermal Video

Pavement Temp.	Calibration Model	R ²	MRE	RAE	RPE
0°C- 5°C	$y = x + 2.50$	0.930	0.103	0.105	0.047
20°C-25°C	$y = x + 0.20$	0.870	0.061	0.005	0.061
25°C-30°C	$y = x + 1.52$	0.770	0.066	0.039	0.056
30°C-35°C	$y = x + 2.88$	0.830	0.106	0.087	0.046
35°C-40°C	$y = x + 2.63$	0.930	0.103	0.126	0.114
40°C-45°C	$y = x + 2.48$	0.900	0.087	0.081	0.058

CONCLUSIONS

This paper presents an approach to integrate and evaluate the performance of thermal and visible light videos for the automated collection and traffic data extraction under various lighting and temperature conditions in urban intersections with high pedestrian and bicycle traffic. The two technologies were

evaluated in terms of road user detection, classification, and vehicle speed estimation. Considering the above results, several key conclusions are drawn.

- 1) The regular camera only narrowly outperformed the thermal camera in terms of detection and classification of all road users during daytime conditions. Also, the regular camera detects and classifies vehicles adequately under nighttime conditions. However, the performance of the regular camera deteriorates for pedestrians and cyclists in all nighttime test cases, while miss rate by the thermal camera remained around 5 %, showing stability across the tested conditions.
- 2) Based on the results at the individual level from the two test cases, the two cameras performed similarly in the favorable case; while for the night, low visibility case, the advantage of using thermal camera was more significant compared to the results at the group level.
- 3) Training of the classifier to account for variation in the appearance of road users in the thermal video was observed to increase classification performance (recall, precision, and global accuracy) for the thermal camera, particularly at higher temperatures. Training the algorithm using more thermal videos is expected to improve the classification performance by thermal video also during the day, where the thermal camera was slightly inferior to regular video.
- 4) Speed measurements by the thermal camera were consistently more accurate than measurements by the regular video. Additionally, speed measurement accuracy was observed to be generally insensitive to lighting and temperature conditions.

Summarizing these points, regular video works well for “overcast” and “sun, little shadow” conditions without lighting interference such as shadow, glare, low visibility, or reflection. The thermal camera performs similarly in these conditions (although classification must be improved by training the algorithm on thermal data). However, with shadows or at night, the performance of the regular camera was greatly reduced, and the thermal camera was superior in terms of detection, classification, and vehicle speed measurement. The thermal videos are insensitive to lighting interference, and solve the issues associated with visible light cameras for traffic data collection, especially for active road users such as pedestrians and cyclists. The thermal camera is also generally insensitive to the effects of pavement temperature. Thermal videos are more reliable and stable compared to regular videos in an around-the-clock collection campaign. Furthermore, greyscale thermal videos with lower resolution provide comparable results during the day, yet require less storage space and processing power, which are key concerns. Finally, thermal videos cause no privacy issues, which are a major hurdle for the application of video-based sensors, especially in the U.S. and European countries.

As part of its contributions, this paper provides an approach for integrating existing tracking and classification algorithms for automated thermal video collection and analysis under varied lighting and weather conditions. The proposed approach can be used for automated counting, speed studies and surrogate safety analyses in particular during low visibility conditions and in environments with high pedestrian and bicycle traffic activity.

Though general improvement of the classification performance was achieved by training the classifier on thermal data, the results (average 83.4 % global accuracy over all cases, in TABLE 6) are lower than what has been reported previously for regular videos (93.3 %) (Zangenehpour^a et al., 2015). Reasons for this reduced performance must be considered in future work, including lower resolution of thermal videos, and the need for more training image samples of road users under different temperature conditions. Validation of the classification algorithms on thermal videos will be better characterized using the ROC curve to compare different methods over several parameter settings. Although past literature shows visual improvements when using thermal cameras in foggy conditions, no work has been done to quantify the improvement of thermal videos during adverse weather

conditions. The evaluation of thermal video in adverse weather conditions, such as heavy precipitation and fog, is a key focus of future work. Finally, a hybrid system that combines the advantages of both technologies can be designed to automatically calibrate and process video data from both thermal and visible spectrum sensors.

REFERENCES

- Anderson-Trocme, P., Stipancic, J., Miranda-Moreno, L., & Saunier, N. (2015). Performance Evaluation and Error Segregation of Video-collected Traffic Speed Data. *Transportation Research Board Annual Meeting*. Washington DC.
- Bahler, S. J., Kranig, J. M., & Minge, E. D. (1998). Field Test of Nonintrusive Traffic Detection Technologies. *Transportation Research Record: Journal of the Transportation Research Board*(1643), 161-170.
- Balsys, K., Valenvicius, A., & Eidukas, D. (2009). Urban Traffic Control Using IR Video Detection Technology. *Electronics and Electrical Engineering*(8), 43-46.
- Bernardin, K., & Stiefelhaven, R. (2008). Evaluating Multiple Object Tracking Performance: The CLEAR MOT Metrics. *EURASIP Journal on Image and Video Processing*, 2008, 1-10.
- Cho, Y., & Rice, J. (2006). Estimating Vehicle Fields on a Freeway from Low-resolution Videos. *IEEE Transactions of Intelligent Transportation Systems*, 7(4), 463-469.
- Coifman, B. (2005). Freeway Detector Assessment: Aggregate Data from Remote Traffic Microwave Sensor. *Transportation Research Record*(1917), 150-163.
- Coifman, B., Beymer, D., McLauchlan, P., & Malik, J. (1998). A Real-time Computer Vision System for Vehicle Tracking and Traffic Surveillance. *Transportation Research Part C*(6), 271-288.
- FLIR Systems, Inc. (2015). *FLIR ONE is Lightweight, Easy to Connect and Easy to Use*. Retrieved from FLIR: <http://www.flir.com/flirone/content/?id=62910>
- FLIR Systems. Inc. (2014). *FLIR ONE User Manual*. Retrieved from <http://www.flir.com/flirone/press/FLIR-ONE-User-Manual.pdf>
- Fu, T., Zangenehpour, S., St-Aubin, P., Fu, L., & Miranda-Moreno, L. F. (2015, May). Using Microscopic Video Data Measures for Driver Behavior Analysis during Adverse Winter Weather: Opportunities and Challenges. *Journal of Modern Transportation*, 23(2), 81-92.
- Huang, H., Zegeer, C., & Nassi, R. (2000). Effects of Innovative Pedestrian Signs at Unsignalized Locations - Three Treatments. *Transportation Research Record*(1705), 43-52.
- Iwasaki, Y. (2008). A Method of Robust Moving Vehicle Detection for Bad Weather Using an Infrared Thermography Camera. *Proceedings of the 2008 International Conference on Wavelet Analysis and Pattern Recognition*, (pp. 86-90). Hong Kong.
- Iwasaki, Y., Kawata, S., & Nakamiya, T. (2013). Vehicle Detection Even in Poor Visibility Conditions Using Infrared Thermal Images and Its Application to Road Traffic Flow Monitoring. In T. Sobh, & K. Elleithy (Eds.), *Emerging Trends in Computing, Informatics, Systems Sciences, and Engineering* (pp. 997-1009). New York: Springer Science+Business Media.
- Krotosky, S. J., & Trivedi, M. M. (2007). On Color-, Infrared-, and Multimodal-Stereo Approaches to Pedestrian Detection. *IEEE Transactions on Intelligent Transportation Systems*, 8(4), 619-629.

- MacCarley, C. A., Hemme, B. M., & Klein, L. (2000). *Evaluation of Infrared and Millimeter-wave Imaging Technologies Applied to Traffic Management*. Society of Automotive Engineers.
- Robert, K. (2009). Night-Time Traffic Surveillance A Robust Framework for Multi-Vehicle Detection, Classification and Tracking. *Advanced Video and Signal Based Surveillance*, (pp. 1-6).
- Sangnoree, A., & Chamnongthai, K. (2009). Robust Method for Analyzing the Various Speeds of Multitudinous Vehicles in Nighttime Traffic Based on Thermal Images. *Computer Sciences and Convergence Information Technology. ICCIT '09. Fourth International Conference*, (pp. 467-472).
- Saunier, N. (n.d.). *Traffic Intelligence*. Retrieved from <https://bitbucket.org/Nicolas/traffickingintelligence/>
- Saunier, N., & Sayed, T. (2006). A Feature-based Tracking Algorithm for Vehicles in Intersections. *IEEE*.
- Shi, J., & Tomasi, C. (1994). Good Features to Track. *CVPR 1994*, (pp. 593-600).
- Thi, T. H., Robert, K., Lu, S., & Zhang, J. (2008). Vehicle Classification at Nighttime Using Eigenspaces and Support Vector Machine.
- VideoLAN Organization. (n.d.). *VideoLAN*. Retrieved from <http://www.videolan.org/vlc/index.html>
- Xu, F., Liu, X., & Fulimura, K. (2005). Pedestrian Detection and Tracking With Night Vision. *IEEE Transactions on Intelligent Transportation Systems*, 6(1), 63-71.
- Yoneyama, A., Yeh, C.-H., & Kuo, C.-C. J. (2005). Robust Vehicle and Traffic Information Extraction for Highway Surveillance . *EURASIP Journal on Applied Signal Processing*(14), 2305-2321.
- Zangenehpour^a, S., Miranda-Moreno, L. F., & Saunier, N. (2015, July). Automated Classification Based on Video Data at Intersections with Heavy Pedestrian and Bicycle Traffic: Methodology and Application. *Transportation Research Part C: Emerging Technologies*, 56, 161–176.
- Zangenehpour^b, S., Miranda-Moreno, L. F., & Saunier, N. (2015). Video-based Automatic Counting for Short-term Bicycle Data Collection in a Variety of Environments. *Transportation Research Board 94th Annual Meeting*. Washington D.C.
- Zangenehpour, S., Strauss, J., Miranda-Moreno, L. F., & Saunier, N. (2016). Are Intersections with Cycle Tracks Safer? A Control-case Study based on Automated Surrogate Safety Analysis using Video Data. *Accident Analysis and Prevention*, 86, 161-172.